After-Fracture Redundancy of Two-Girder Bridge: Testing I-40 Bridges Over Rio Grande

R. L. Idriss, K. R. White, C. B. Woodward, and D. V. Jauregui,
New Mexico State University

The I-40 bridges over the Rio Grande in Albuquerque, New Mexico, were due to be razed in the fall of 1993 because of geometry and traffic safety considerations, thus providing a unique opportunity for testing them. These medium-span steel bridges represent a common design in the United States and are classified by AASHTO as nonredundant "fracture critical" two-girder steel bridges ("fracture critical" classification means that failure of a primary member would probably cause collapse of the bridge. The subject bridge, built in 1963, is 1,275 ft (390 m) long and consists of three medium-span continuous units with spans of 131, 163, and 131 ft (40, 50, and 40 m) each. The bridge was field tested to determine the impact of a near full-depth girder fracture on the redistribution of loads, the load capacity, and the potential for collapse. Four levels of damage were introduced in the middle span of the north plate girder by making various cuts in the web and the flange of the girder. The final cut resulted in a crack 6 ft (1.8 m) deep in the 10-ft (3.1-m)-deep girder, extending from the bottom flange to the floor beam to girder connection. Data were taken under dead load and under a static live load consisting of an 82,000-lb (365,000-N) truck. The fractured bridge proved to be stable, with minimal deflection and no yielding. The after-fracture response and the load redistribution in the fractured bridge were evaluated. The contribution of the various members to the redundancy of the structure was assessed.

The I-40 bridges over the Rio Grande in Albuquerque were due to be razed in mid-1993 because of geometry and traffic safety considerations. The bridges represent a common design in the United States and are classified as nonredundant "fracture critical" two-girder steel bridges. AASHTO's Standard Specifications for Highway Bridges (*1*) defines nonredundant load path structures as "structure types where failure of a single element could cause collapse." The two-girder bridge design, using welded steel plate girders as the primary structural elements was a popular design in the 1950s and 1960s. A large number of these bridges are currently in service around the United States. These bridges have fatigue-sensitive details and are nearing the limit to their practical fatigue life. In a number of instances, cracks developed in the webs, flanges, secondary members, and connections, resulting in uncertainty about the integrity of these bridges and their safety and creating concern for the practicing bridge engineer.

Experience shows that two-girder highway bridges typically do not collapse when a fracture occurs in a girder. In many instances, they remain serviceable, and damage sometimes is not even suspected until the fracture is discovered incidentally or during inspection (*2,3*). Much still needs to be learned about the after-fracture behavior of these structures and how the load gets redistributed when fracture occurs. The main ob-

jective of the testing was to investigate the behavior of the fractured bridge and the after-fracture redundancy present in the structure. This paper reports on the redundancy present in a fractured two-girder steel bridge.

Bridge Description

The structure, built in 1963, is a 1,275-ft (390-m) long, noncomposite bridge consisting of three-span continuous units with spans of 131, 163, and 131 ft (40, 50, and 40 m) each. The structural unit is a two-girder design welded with bolted splices with a floor system (Figures 1 through 3).

Analytical Model

A preliminary analytical study (*4*) was needed for (*a*) safety consideration and (*b*) gauge placement. A three-dimensional finite element computer model of the bridge was developed (*4*). (Figure 4). A full description of the finite element model appears elsewhere (*4*). The results of this analytical study (*4*) were used to (*a*) evaluate after-fracture behavior and choose defects to implant on the bridge; (*b*) determine the sensor locations and optimize the quality and quantity of the data acquisition devices; and (*c*) calculate the load on the jacks during temporary shoring, the clearance needed at the cut, and the positioning of the truck for static loading.

The preliminary analysis of the structure with a near full-depth crack at midspan of the central span predicted a stable structure, with minimum deflections, and no yielding. The following behavior was observed:

1. Most of the load was observed to be redistributed longitudinally via the north damaged girder to the interior supports, as demonstrated by the large increase in negative moment at the interior supports after fracture (Figure 5), and
2. Some of the load was redistributed in the transverse direction to the intact girder because of the torsional rigidity of the deck, floor beam, and bracing system as shown by the increase in positive moment at midspan of the central span (Figure 6).

Bridge Monitoring: Placement of Strain Gauges

On the basis of the preliminary finite element analysis and load path evaluation, the focus of this study was on monitoring the elements that showed the most significant change in load. The following were mainly monitored:

1. The moment in the north (damaged) girder at the interior girder supports;
2. The moment in the south (intact) girder at midspan and at the interior supports;
3. Forces in the bracing at the vicinity of the crack, because the analytical model predicted a large increase in the bracing load at the crack zone;

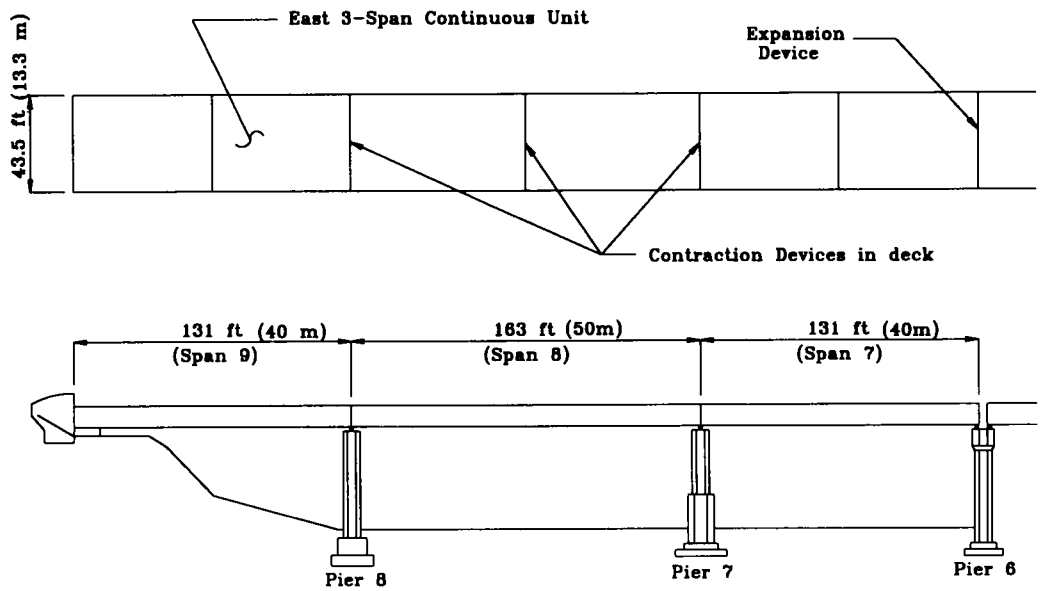

FIGURE 1 Overall plan and elevation of east three-span continuous unit of eastbound I-40 bridge.

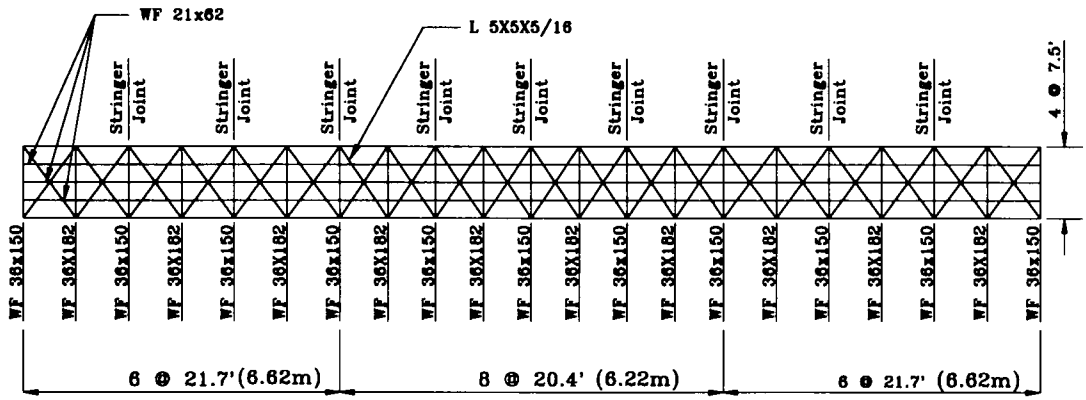

FIGURE 2 Plan view of steel superstructure below bridge deck.

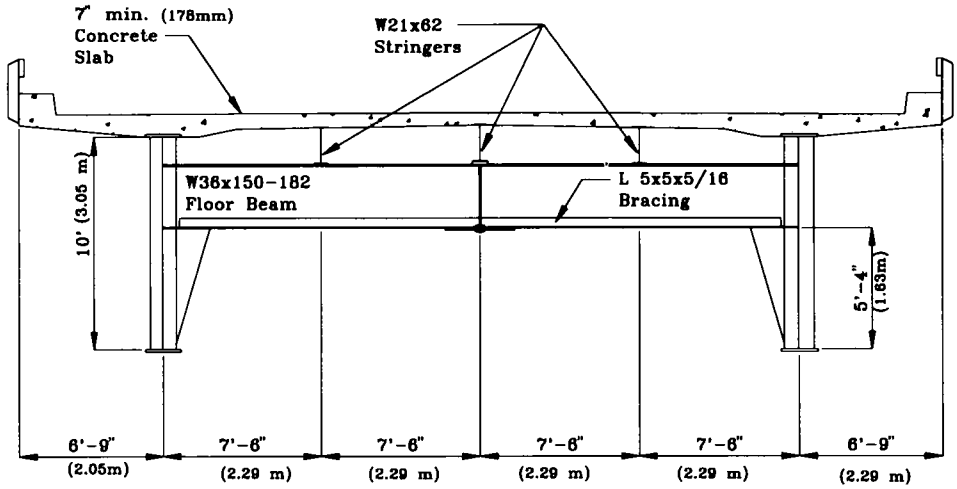

FIGURE 3 Cross section of I-40 bridge at floor beam location.

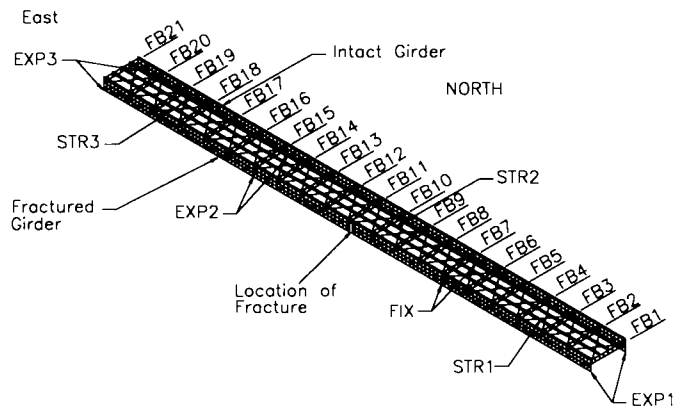

FIGURE 4 Finite element model of I-40 bridge (below reinforced concrete deck).

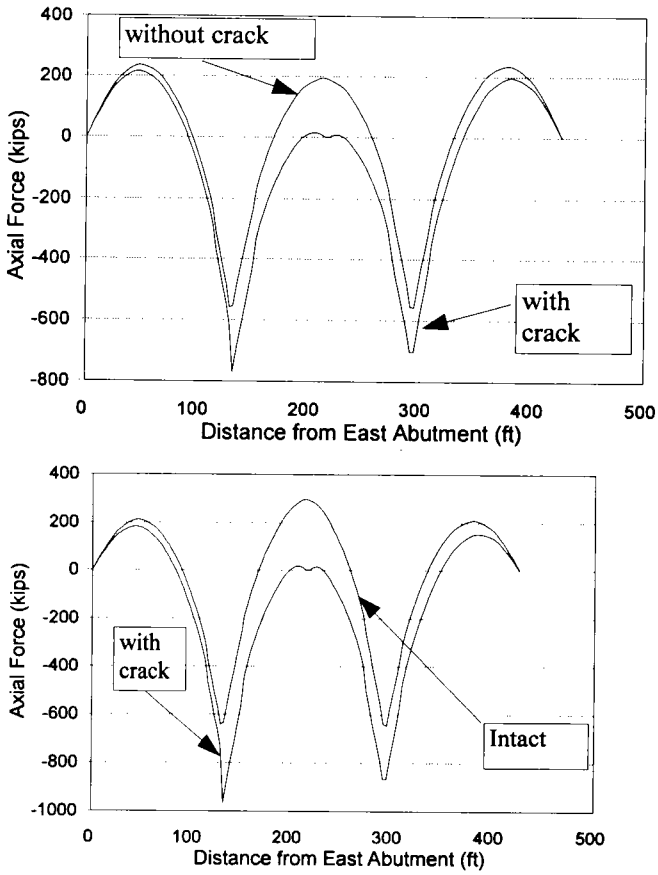

FIGURE 5 *Top*: North girder bottom flange forces; *bottom*: north girder bottom flange forces under dead load plus two HS-20 truck loadings, no impact (1 kip = 4.45 kN, 1 ft = 0.305 m).

4. Moments in floor beams at midspan and at the connection to the intact girder. It was anticipated that the floor beams at the vicinity of the crack would transfer load to the intact girder through cantilever action and develop a negative moment at their connection to the intact girder as they cantilever toward the crack; and

5. The load increase in the stringers. For this gauges were placed on the bottom flange of the middle stringer and the stringer closest to the north girder fracture (the stringer at the most remote location to the damage was not monitored).

The strain gauge locations are shown in Figures 7 through 11. Encapsulated, self-compensated, 1/4-in. (6.35-mm) metal foil gauges were used (Micro Measurements CEA-06–250UW-305). The deflection was measured at various locations on the north and south girders, particularly at midspan of the west exterior span and at midspan of the central span.

Bridge Testing (*5*)

Static Tests

A general tractor-trailer with a front-to-back axle spacing of 55.18 ft (16.82 m) and weighing 81,620 lb (363 100 N) was furnished by the New Mexico State Highway and Transportation Department for the static tests. The layout and magnitude of the wheel loads are provided in Figure 12. With this configuration, the truck was found to be 95.5 percent of the maximum New Mexico legal load and roughly equivalent to an HS-18.35 in the positive moment region of the test bridge. At this location, it gave maximum positive moment at midspan of the central span and almost maximum negative moment at the interior supports. Influence line studies were used to position the truck.

1. For maximum positive moment at midspan of the central span and almost maximum negative moment at

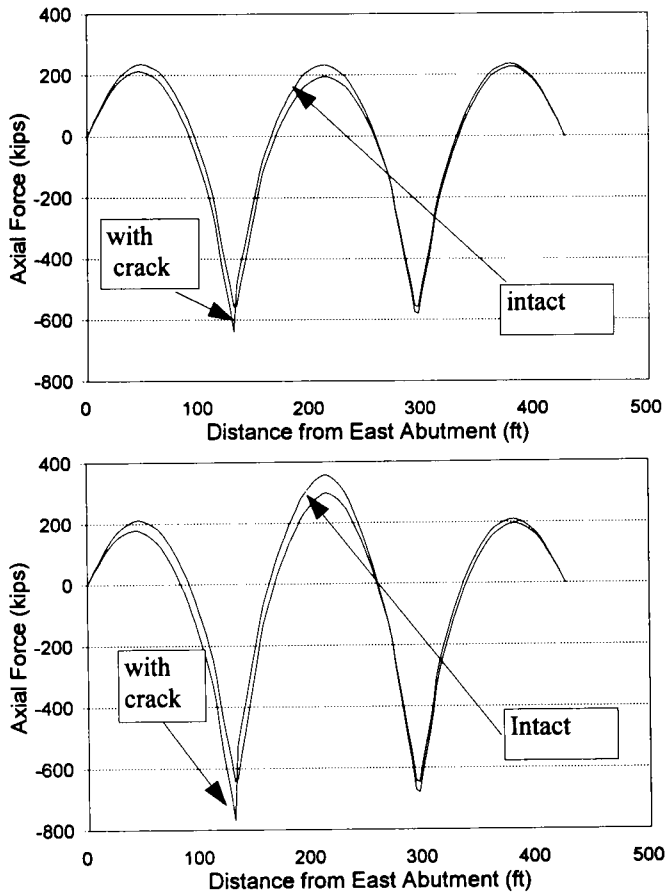

FIGURE 6 *Top*: south girder bottom flange forces under dead load; *bottom*: south girder bottom flange forces under dead load plus two HS-20 truck loadings, no impact (1 kip = 4.45 kN, 1 ft = 0.305 m).

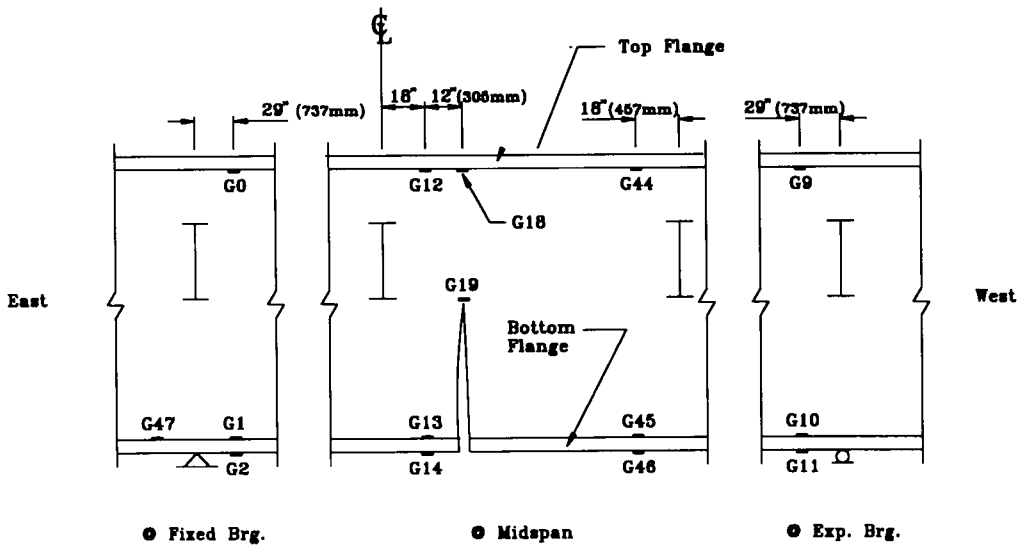

FIGURE 7 Positioning of strain gauges on north (damaged) girder (view from inside looking out).

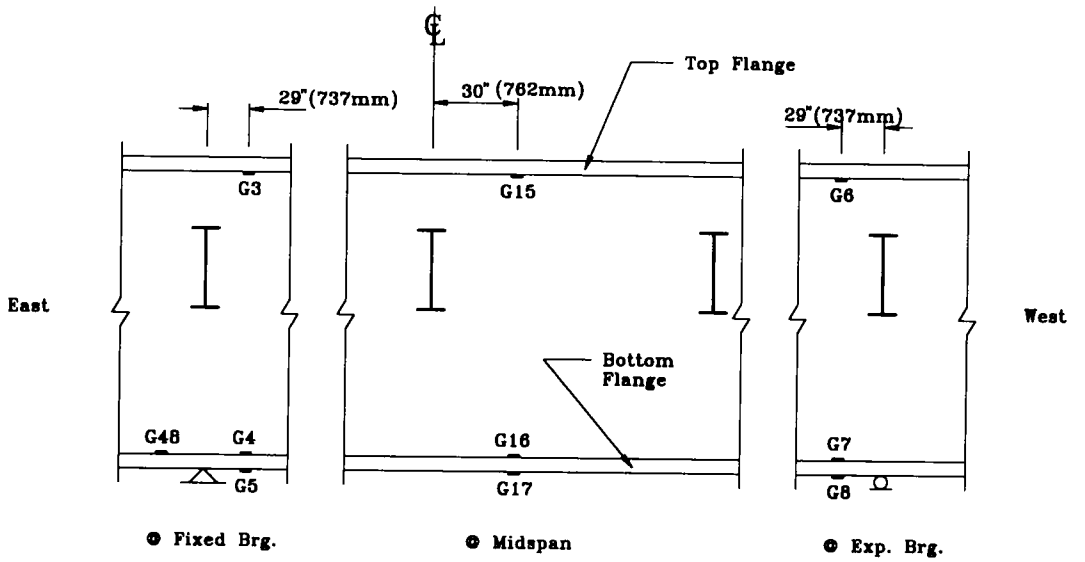

FIGURE 8 Positioning of strain gauges on south (intact) girder (view from inside).

the interior supports, the third axle of the truck was placed at midspan of the central span

2. For minimum moment at midspan of the central span and large moment at the west interior support, the third axle of the truck was placed 75 ft (22.88 m) from the west end of the three-span unit.

Strain gauge zeroing measurements were to be taken with the structure unloaded. Readings were then taken with the third axle of the truck stopped at the above-mentioned locations on the north driving lane. This general procedure was repeated for the pristine structure and for the damaged bridge at each stage of the cuts. In addition, strain readings were taken under dead load before and after the flange cuts. Deflection measurements were scheduled to be taken simultaneously with the strain readings. Temporary shoring was positioned below the cut for safety considerations. The support tower was also used for access, as a platform for jacking up the north girder to relieve stress in the bottom flange before the final flange cut and for splicing the flange cut after the testing.

Damage Description

Four different levels of damage were introduced in the middle span of the north plate girder by making various torch cuts in the web and the flange of the girder. This occurred from September 3–8, 1993. The final cut was to simulate a near full-depth crack in the girder. This type of crack, usually a fatigue crack, develops at

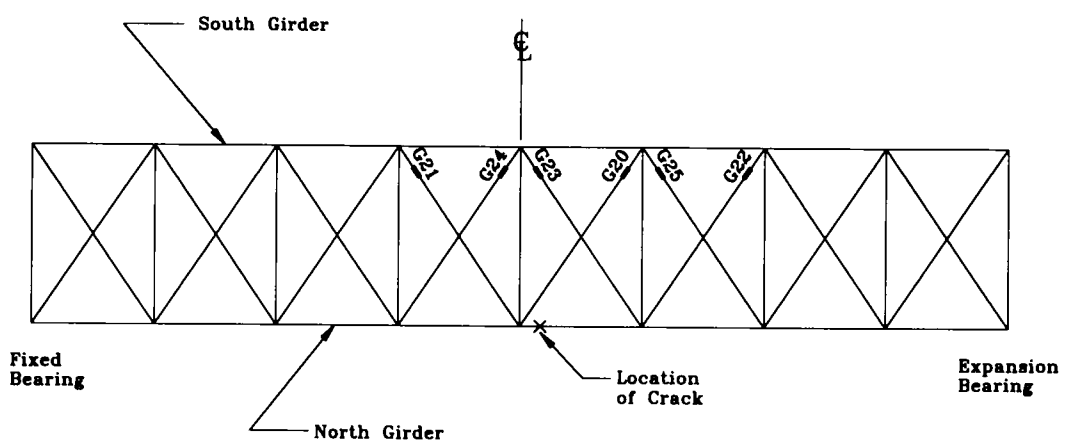

FIGURE 9 Positioning of strain gauges on lateral bracing system (top view).

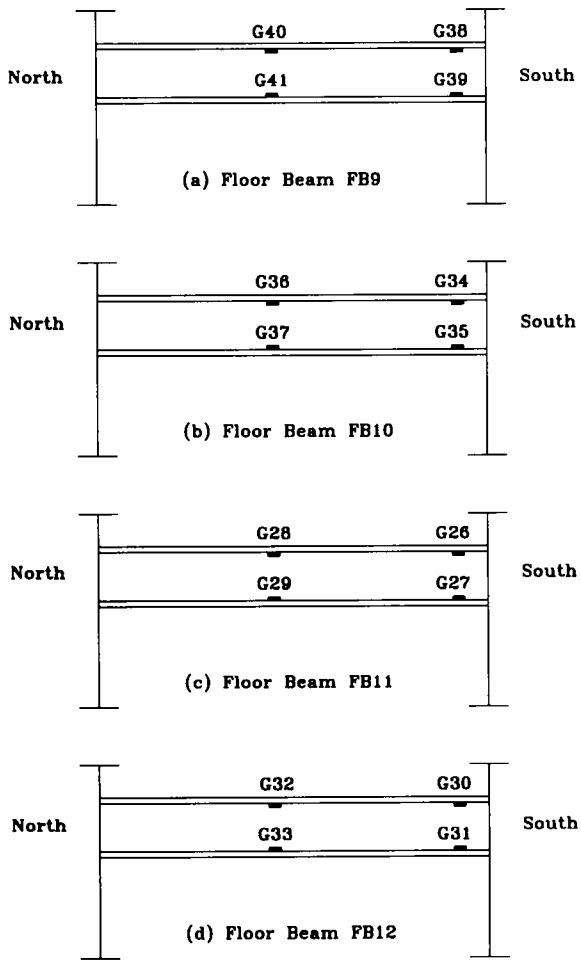

FIGURE 10 Positioning of strain gauges on floor beams.

fatigue-sensitive details in the bridge, often at the girder-to-floor beam connection because of out-of-plane bending of the web. The cut in the girder was done in four stages. Damage was to be inflicted on the bridge by a series of cuts, near midspan of the central span of the north girder 2.5 ft (0.762 m) west of the center of the bridge, midway between two vertical stiffeners. The first-stage cut was a cut in the web 2 ft (0.61 m) deep, originating at the floor beam connection level. Next the cut was continued to the bottom of the web. During this cut of the web, the web bent out of plane approximately 1 in. (25.4 mm). The third stage was to cut the flange halfway in from each side, directly below the web cut. Finally, in the fourth stage, the flange was severed completely, leaving the upper 4 ft of the web and the top flange to carry load at that location.

For the final cut, the north girder was blocked up and jacked upward ½ in. (12.7 mm) to relieve dead load stress in the flange. Computer predictions required the girder to be jacked up ¾ in. (19.1 mm) to relieve the bottom flange stress; however, the wooden blocks beneath the jacks began to crack at about ½ in. (12.7 mm). It was decided that ½ in. (12.7 mm) was enough to alleviate the force in the bottom flange and to allow a safe final cut.

The bottom flange was then severed entirely and the girder was slowly lowered until no contact existed between the jacks and the flange. The final cut resulted in a crack 6 ft (1.83 m) in the 10-ft (3.1-m)-deep girder, extending from the bottom flange to the floor beam to girder connection.

Using the support tower as a reference level, the distance to the bottom flange was measured before and after the final flange cut. The difference of the two measurements represented the added deflection of the

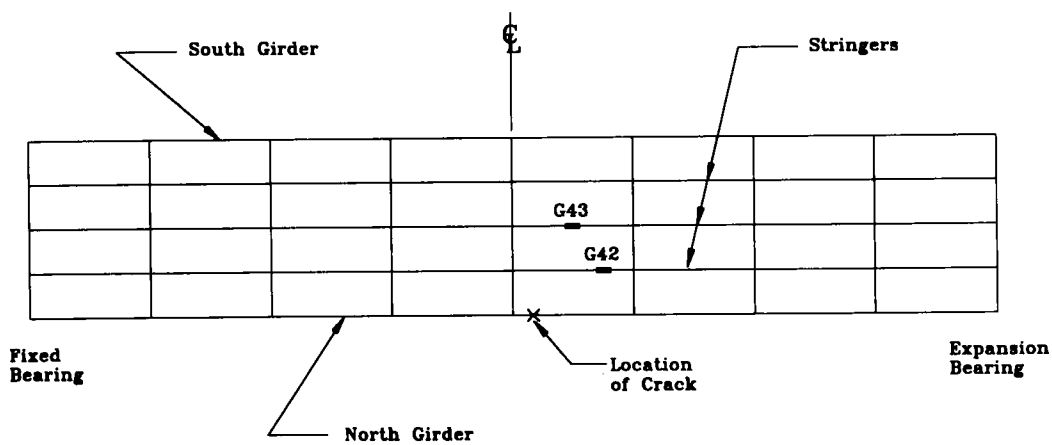

FIGURE 11 Positioning of strain gauges on stringers (top view).

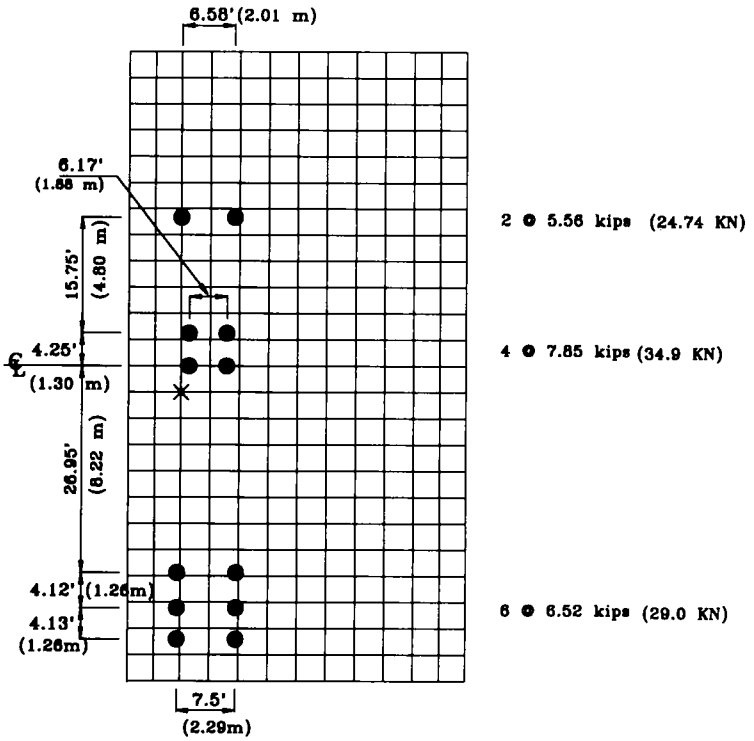

FIGURE 12 Application of HS-18.35 truck to bridge deck.

north girder caused by the mid-depth fracture under dead load. Utilizing this approach, the bottom flange of the girder at the cut deflected by only $^{11}/_{16}$ in. (17.5 mm), and the crack opened $^{3}/_{8}$ in. (9.52 mm).

When the truck was positioned above the cut, the crack opened to $^{3}/_{4}$ in. (19.1 mm) and the girder deflected by an additional $^{1}/_{2}$ in. (12.7 mm), for a total deflection under dead and live load of $1^{3}/_{16}$ in. (30.2 mm). There were no signs of yielding.

On Thursday, Sept. 9, equipment was removed from the bridge site, and the cut flange was spliced for security during the razing of the bridge.

Strain Gauge Data

There was no significant change in strains experienced by the gauged members during the various stages of damage, as shown in Tables 1 through 5 until the bottom flange was completely severed. This shows that load redistribution did not occur until the bottom flange was completely cut. The only noticeable change throughout the various phases was localized and occurred after the second web cut. During this cut, gauges G13 and G14 located on the bottom flange of the damaged girder, closest to the fracture, experienced a surge in tension (Table 1). This shows that the web plus half flange fracture did not alter the bridge stiffness enough to initiate load transfer. It is not until the flange is totally severed that the load redistribution occurs.

Load Redistribution

North (Damaged Girder)

The after-fracture strain readings show that the north girder is the dominant redundant load path. Continuity at the interior supports allowed the girder to redistribute the load longitudinally through cantilever action to the interior supports. This is shown by the significant increase in negative moment at the interior supports as shown by the surge in compression force in the bottom flange of the north girder at the interior supports. This is evident by the large negative changes in strain recorded for the gauges positioned at the fixed support (G2) and at the expansion bearing (G11) as shown in Table 1. The largest strain measured in the structure was measured at the interior supports of the damaged girder. The live load stresses measured at G2 and G11 were 1.32 ksi and 1.50 ksi, respectively. The predicted live load stress at these locations by the finite element model was at 2.0 ksi, which proved to be conservative. The predicted dead load stress (finite element model) was 13 ksi. The total dead and live load stress was 15

TABLE 1 North (Damaged) Girder: Strain Readings Under Truck Loading at Central Span in Microinches per Inch

	No Damage	1st Web Cut	2nd Web Cut	1st Flange Cut	Final Cut
Gage G2 @ Fixed Bearing	-30.9	-30.8	-31.1	-31.5	-46.2
Gage G11 @ Expansion Bearing	-35.4	-35	-35	-35.9	-51.6
Gage G13 @ cut	89.5	89.3	110	122	0
Gage G14 @ cut	87.4	87.8	133	135	0

TABLE 2 Stringers: Strain Readings Under Truck Loading at Central Span in Microinches per Inch

	No Damage	1st Web Cut	2nd Web Cut	1st Flange Cut	Final Cut
STR1 G42	-5.5	-5.0	-5.8	-6.5	2.9
STR2 G43	-0.3	1.8	1.8	1.4	14.9

TABLE 3 South Intact Girder: Strain Readings Under Truck Loading at Central Span in Microinches per Inch

	No Damage	1st Web Cut	2nd Web Cut	1st Flange Cut	Final Cut
G5 (Fixed Bearing)	-3.7	-3	-3.3	-3.2	-2.6
G8 (Expansion Bearing)	-5.5	-4.4	-4.8	-4.9	-5
G17 (Midspan)	19	18.3	17.6	17.4	23.4

TABLE 4 Floor Beams: Strain Readings Under Truck Loading at Central Span in Microinches per Inch

	No Damage	1st Web Cut	2nd Web Cut	1st Flange Cut	Final Cut
FB9 Gage G39	-1.0	-1.1	-1.1	-0.9	1.7
FB10 Gage G35	-3.9	-4	-4.5	-4.5	-6.9
FB11 Gage G27	-7.1	-7.6	-7.9	-7.9	-23.6
FB12 Gage G31	-3.8	-3.9	-3.7	-3.2	-3.3

TABLE 5 Bracing: Strain Readings Under Truck Loading at Central Span in Microinches per Inch

	No Damage	1st Web Cut	2nd Web Cut	1st Flange Cut	Final Cut
Panel East of Crack					
G21	.8	-1.6	-2.0	-2.1	-24.9
G24	28.4	26.2	28.6	30	68.0
Panel @ Crack					
G20	8.5	8.1	9.6	10.5	15.5
G23	20.8	19.2	21.2	21.5	57.0
Panel West of Crack					
G22	-16.5	-19.3	-19.8	-19.7	-58.1
G25	36.2	37.2	37.5	38.3	68.5

ksi, less than the inventory stress level recommended by AASHTO (0.55 times the yield stress) of 20 ksi.

Stringer-Deck System

After fracture, load is shed to the stringer-deck system. The after-fracture strains (Table 2) recorded for gauges G42 and G43 showed the stringers to be carrying more load. In addition, the longitudinal gauge positioned on the bridge deck showed a large surge in compression following the crack.

South Girder

The intact girder has an increase in positive moment at midspan as indicated by the positive change in strain recorded at that location by Gauge G17 (Table 3). A 20 percent increase in tension in the bottom flange at midspan was measured under live load.

Floor Beams

As predicted, the floor beams at the vicinity of the crack redistributed the load to the intact girder. The most drastic change occurred in floor beam FB11 located at the crack. It acted essentially as a cantilever beam because of the lack of support from the damaged girder. This cantilever action is demonstrated by the increase in negative moment at the connection with the intact girder as indicated by the strain measurements at that location (Table 4). Floor beam FB10, located directly west of the crack, also experienced an increase of negative moment at its south end, but not as much as floor beam FB11. The other two floor beams located in the crack zone but further away from the crack, FB9 and FB12, do not show a significant change in behavior.

Lateral Bracing System

Strain readings show a large increase in the load carried by the diagonals (Table 5). There also was a change in load patterns for the lateral bracing. The two diagonals in the bay at the crack were both in tension and experienced a drastic increase in their tensile force (strain measured after fracture was two to three times the strain measured before fracture). Because of twisting in the structure, in the panel east of the crack, one of the diagonals increased in tension while the other went from tension to compression.

Role of the Deck

Longitudinal as well as transverse load redistribution is provided by the deck. After-fracture strains recorded under dead load with the deck rosette are provided in Table 6. The table gives the results gathered during the last two stages of girder cuts. The longitudinal gauge, which was positioned on the bridge deck above the middle stringer, recorded a large surge of compression on completion of the final flange cut. The transverse gauge placed at the same location as the longitudinal gauge indicated an increase in tension in the deck. Before the crack, the deck acts as a continuous beam over the stringers in the transverse direction. When the crack is imposed, the north portion of the bridge near the crack sags downward. Like the floor beams at that location, the deck cantilevers out from the higher supported areas on the south end. This is indicated by an increased tension experienced by the deck in the transverse direction.

Conclusions

When a mid-depth fracture was imposed on the north girder of the three-span unit, it changed the bridge into a new but still stable structure. Deflection at the crack was minimal at $1\frac{3}{16}$ in (30.2 mm) under dead plus live loading, and there was no yielding. The load redistribution was provided in the three-dimensional structure by both primary and secondary members via the deck, stringers, floor beams, and bottom lateral bracing. Most of the load was redistributed longitudinally through the damaged girder and stringer deck system to the interior supports. The main load path proved to be the fractured girder itself as it redistributed the load longitudinally to the interior supports through cantilever action. The floor beams, lateral bracing system, and deck transferred the load to the intact girder, through torsional stiffness of the system. This load transfer in the transverse direction occurred mainly at the vicinity of the crack.

TABLE 6 After-Fracture Strains in Deck Under Dead Load in Microinches per Inch

Gage	First Flange Cut	Final Flange Cut
Longitudinal	-5.5	-138
Transverse	2.6	17.2
@ 45 degrees	-5.4	-47.4

Further Research

The following recommendations are suggested to extend the reported research:

1. Investigate the after-fracture behavior of the bridge with a crack at midspan of an exterior span. This fracture scenario could prove to be more critical than the fracture at midspan of an interior span because the cantilever action provided by the interior supports will not be available at the abutment.
2. Investigate the possible loss of composite action between the girder and the deck with increasing loading.
3. Develop nondestructive monitoring systems for this family of bridges. On the basis of the bridge testing results, this monitoring system can be effective and can focus on the critical zones.

ACKNOWLEDGMENT

This study is part of the overall testing of the I-40 Bridge, in Albuquerque, New Mexico. It was funded by a grant from the National Science Foundation, the New Mexico State Highway and Transportation Department, FHWA, and the New Mexico Alliance for Transportation.

REFERENCES

1. *Standard Specifications for Highway Bridges*, 13th ed. AASHTO, Washington, D.C., 1983.
2. Daniels, J. H., W. Kim, and J. L. Wilson. *NCHRP Report 319: Recommended Guidelines for Redundancy Design and Rating of Two Girder Steel Bridges*. TRB, National Research Council, Washington, D.C., 1989.
3. Schwendeman, L. P., and A. W. Hedgren. Bolted Repair of Fractured I-79 Girder. *Journal of the Structural Division* ASCE, Vol. 104, No. ST10, Oct. 1978, pp. 1567–1669.
4. Idriss, R. L., and D. V. Jauregui. *Load Path Evaluation of the I-40 Bridge*. Report 94-01 to the National Science Foundation. Department of Civil Engineering, New Mexico State University, April 1994.
5. White, K. R., and J. Minor. *Testing of the I-40 Bridge*. Phase 1 Final Report. FHWA, U.S. Department of Transportation, 1994.